

Measurement of intrinsic fluorescence to probe the conformational flexibility and thermodynamic stability of a single tryptophan protein entrapped in a sol–gel derived glass matrix

Lili Zheng and John D. Brennan*

Department of Chemistry, Brock University, St. Catharines, ON, Canada L2S 3A1.
E-mail: jbrennan@chemiris.labs.brocku.ca

In this study techniques based on measurement of intrinsic tryptophan (Trp) fluorescence were used to monitor the stability and conformational flexibility of the single tryptophan protein monellin which was entrapped in sol–gel derived glass monoliths formed from tetraethylorthosilicate. The monoliths were aged either in buffer (wet-aged) or in air (dry-aged). The steady-state fluorescence spectra, steady-state anisotropy and acrylamide quenching behaviour of the single Trp at position 3 were monitored during chemical denaturation with guanidine hydrochloride, and during thermal denaturation. These studies indicated that there were no significant improvements in either chemical or thermal stability when the protein was present in wet-aged monoliths. However, the long-term stability of the protein was improved six-fold when such monoliths were stored at 4 °C. The encapsulation of monellin into dry-aged monoliths caused the thermal unfolding transition to broaden and shift upward by 10 °C, and caused the long-term stability to improve by 12-fold (compared to solution). Chemical stability studies also showed a broader transition for the unfolding of the protein in dry-aged monoliths, and suggested that the protein was present in a distribution of environments, each with a slightly different thermodynamic stability. The steady-state fluorescence responses obtained during denaturation and the accessibility of native and denatured protein to quencher provided clear evidence that the entrapped protein had a smaller range of conformational motions compared to the protein in solution, and that the entrapped protein was not able to unfold completely. The restriction of conformational motion, along with the increased structural order of the internal environment of the monoliths, play a role in the improvements in thermal and long-term stability that were observed.

Keywords: Protein; sol–gel; biosensor; fluorescence; stability

In the past few years, several groups have reported on the development of analytical devices utilizing biological components that were encapsulated in an inorganic silicate matrix formed by a low temperature sol–gel processing method.^{1–3} An important finding with regard to the utilization of these materials for sensors was that biomolecules were usually entrapped with the retention of a substantial fraction of their initial activity.³ In addition, many reports suggested that protein stability was actually improved upon entrapment.^{1,4} These findings resulted in several studies which were aimed at understanding the structure and dynamics of entrapped proteins,⁵ the internal environment of sol–gel derived matrices,⁶ and the overall basis for the enhancement in long-term protein stability.³ In spite of the amount of work done, the structure and

environment of entrapped proteins and the basis for the improved stability are still not well understood.

The measurement of the fluorescence of tryptophan (Trp) residues within proteins can be utilized to monitor several parameters, including protein structure,^{7,8} dynamics,⁹ stability,¹⁰ and folding and unfolding phenomena.¹¹ A standard method for examining protein stability in solution is to measure the changes in the fluorescence from intrinsic Trp residues as a function of temperature or denaturant concentration.¹¹ Proteins which contain a single Trp residue are generally used for such studies since they allow for unambiguous investigation of the region being probed, provide a simple system for examining fluorescence lifetimes (which becomes hopelessly complicated if two or more Trp residues are present), and also provide a simpler system for probing rotational anisotropy or exposure of Trp to quenchers. Tryptophan fluorescence has also been used to examine the kinetics of reactions involving proteins which were either in solution¹² or entrapped in a sol–gel derived matrix,¹³ and has recently been used to examine conformational motions and accessibility of entrapped proteins.¹⁴ Hence, tryptophan fluorescence may be used to monitor the interactions between entrapped proteins and analytes.

Recently, we described a method for preparing optically clear monoliths which were suitable for monitoring the fluorescence of Trp residues within encapsulated proteins.¹³ These monoliths were sufficiently thin to permit titrations of an entrapped protein to be done, and allowed for an examination of the interaction between the entrapped single tryptophan protein monellin and external reagents. In this paper, we extend these studies to investigate the thermal and chemical stability of monellin when entrapped in such monoliths. Monellin was chosen for this study for a number of reasons. Firstly, the protein is small, with a molecular weight of 10.7 kDa and a diameter of 3.5 nm.^{15,16} Thus, it is similar in size to a number of small proteins such as cytochrome-*c*^{2,3(a)} and myoglobin¹⁴ which have been studied previously in sol–gel derived monoliths. Secondly, the protein is highly structured, but has no disulfide bridges,¹⁷ indicating that it should be possible to fully unfold the protein using either high temperatures or a high concentration of denaturant. Thirdly, monellin contains only one Trp residue per protein, located in a moderately hydrophobic region near the end of a β -sheet. This makes the interpretation of fluorescence data much simpler since a single segment of the protein can be monitored. Lastly, previous studies of monellin have shown that the intrinsic Trp fluorescence is sensitive to the unfolding of the protein in solution,¹⁸ thus intrinsic fluorescence should be useful for monitoring the stability, structure and conformational motions of the entrapped protein.

This study shows that the fluorescence spectra, steady-state anisotropy and acrylamide quenching of the single Trp residue within monellin can be used to provide useful information about a number of parameters. These include the ability of entrapped proteins to undergo large scale conformational changes; the

changes in thermal, chemical and long term stability which occur upon encapsulation; and the effects of aging the sol-gel derived matrix on the distribution of protein environments. These results are able to provide useful insights into the basis for the changes in protein stability which are observed upon entrapment.

Experimental

Chemicals

Monellin and polymethacrylate fluorimeter cuvettes (transmittance curve C) were obtained from Sigma (Oakville, ON, Canada). Tetraethylorthosilicate (TEOS, 99.999 + %) and acrylamide (99 + %) were supplied by Aldrich (Milwaukee, WI, USA). The guanidine hydrochloride (GdHCl, Sequanol grade) was from Pierce (Rockford, IL, USA). The Sephadex G-25 fine powder was supplied by Pharmacia Biotech (Uppsala, Sweden). All water was twice distilled and deionized to a specific resistance of at least 18 MΩ cm⁻¹ using a Milli-Q 5 stage water purification system (Millipore-waters, Milford, MA, USA). All other chemicals were of analytical reagent-grade and were used without further purification.

Procedures

Preparation of TEOS derived monoliths

The detailed methods used to prepare and characterize sol-gel derived monoliths containing monellin were described previously.¹³ Briefly, a mixture of 4.5 ml of TEOS, 1.4 ml of water and 100 µl of 0.1 M HCl was sonicated for 1 h and stored at -20 °C for 7 to 10 d. A volume of 300 µl of the cold TEOS solution was mixed with an equal volume of cold phosphate buffer (100 mM, pH 7.2, with 100 mM KCl) containing 0–30 µM of protein which had been purified by passage through a column containing Sephadex G-25 resin. The mixture was immediately placed into a disposable acrylate cuvette (1 cm pathlength) which was then sealed with Parafilm and placed on its side until gelation occurred (normally about 1–2 min). The monoliths were then rinsed with buffer several times and were either aged in buffer at 4 °C for a period of 10 d (wet-aged), or in air at 4 °C for 30 d (dry-aged). Aged monoliths were carefully rehydrated by incubating the monoliths in a 100% humidity environment overnight followed by slow immersion into 2 ml of buffer.

Fluorescence measurements in solution

Fluorescence measurements were done using equipment which is described elsewhere.¹³ For fluorescence spectra, samples containing 10 µM of monellin were excited at 295 nm and emission was collected from 305 nm to 450 nm in 1 nm increments at a rate of 180 nm min⁻¹ using a 4 nm bandpass and an integration time of 0.30 s. For all experiments, appropriate 'no protein' blanks were subtracted from each sample and the spectra were corrected for deviations in emission monochromator throughput and photomultiplier tube (PMT) response.

Fluorescence anisotropy measurements were performed in the L-format using Glan-Taylor prism polarizers in both the excitation and emission paths, as described previously.¹³ Single point anisotropy measurements were generally made with excitation at 295 nm and emission at 340 nm, using a 4 nm bandpass and a 3.0 s integration time. The anisotropy values were corrected for the instrumental G factor to account for any polarization bias in the monochromators. These experiments were done with 30 µM of protein to provide sufficient signal with the polarizers in place. All anisotropy values reported are the average of five measurements each on two different samples.

Fluorescence measurements of proteins in monoliths

Rehydrated monoliths, both with and without protein, were carefully mounted in quartz cuvettes at an angle of 45° with respect to the excitation path such that the excitation radiation was reflected away from the emission monochromator and PMT.¹³ Fluorescence spectra were collected from monoliths containing 10 µM of monellin and from monoliths containing no protein using the instrumental configuration described above, and the sample spectra were corrected as described above. Anisotropy values were collected from monoliths containing 30 µM of monellin. The variability in the anisotropy of the blank was very small, and the intensity and anisotropy values of the blanks were usually less than 1% of those obtained from the protein-loaded monoliths, thus no blank subtraction was performed.

Thermal denaturation studies

For solution based studies, a volume of 2.0 ml of monellin in a buffer consisting of 100 mM sodium phosphate, 100 mM KCl, pH 7.2 was placed into a quartz fluorimeter cuvette. For monolith studies, 2.0 ml of the buffer was placed into the cuvettes containing the monolith. All solutions (either containing free monellin or the monolith) were purged with a nitrogen stream for 15 min and immediately capped to remove dissolved oxygen, which was shown to cause irreversible alterations in the fluorescence signals from thermally unfolded proteins.

The temperature was raised in *ca.* 5 °C increments starting at 20 °C and going to 70 °C for solution or wet-aged monoliths and to 80 °C for dry-aged monoliths. The temperature was controlled using a Neslab R110 recirculating water bath, and the temperature of the solution in the cuvette was measured directly using a thermistor probe (Hanna Instruments model 9043A) to account for loss of heat through the Tygon tubing connecting the sample holder and the water bath. The samples were allowed to equilibrate for at least 10 min at each temperature with no stirring. A fluorescence spectrum or anisotropy value was then collected from the sample and an appropriate blank at each temperature. The corrected spectra were integrated from 310 to 450 nm and the intensity at each point was normalized to the intensity at the beginning of the experiment to generate intensity-based unfolding curves. Alternatively, anisotropy values were plotted directly against temperature to generate anisotropy-based unfolding curves.

The unfolding curves were analyzed by non-linear fitting to the equation described by Eftink:¹¹

$$F = \frac{F_{0N} + s_N T + (F_{0U} + s_U T) \exp[-(\Delta H_{un}^0 + T \Delta S_{un}^0) / RT]}{1 + \exp[-(\Delta H_{un}^0 + T \Delta S_{un}^0) / RT]} \quad (1)$$

where F is the measured intensity (or anisotropy) at some temperature T , and R is the gas constant. The remaining six terms were fitting parameters, where F_{0N} and F_{0U} were the fluorescence intensity (or anisotropy) of the native and unfolded states, respectively, s_N and s_U were the baseline slopes of the native and unfolded states as a function of temperature, respectively, and ΔH_{un}^0 and ΔS_{un}^0 were the enthalpy change and entropy change for the unfolding reaction, respectively. The quality of the fit was judged by the chi-squared parameter for the fit. The free energy change for unfolding (ΔG_{un}) was determined by using eqn. 2¹⁹ with a reference temperature (T_r) of 20 °C

$$\Delta G_{un}(T_r) = \Delta H_{un}^0 - T_r \Delta S_{un}^0 + \Delta C_{p,un}[(T_r - T_{un}) - T \ln(T_r/T_{un})] \quad (2)$$

where $\Delta C_{p,un}$ is differential heat capacity for unfolding, and accounts for the temperature sensitivity of the entropy and enthalpy terms on going from T_r to T_{un} .

Chemical denaturation studies

For solution based studies, a volume of 1.30 ml of monellin in buffer was added to a quartz cuvette. A total of 29 aliquots of 8.0 M GdHCl in buffer were added ($4 \times 30 \mu\text{l}$, $12 \times 60 \mu\text{l}$, $13 \times 100 \mu\text{l}$) with constant stirring and a minimum of 10 min was allowed for equilibration (with a shutter blocking the excitation light). A fluorescence spectrum or a steady state anisotropy value was collected at each point from both the sample and a blank containing an identical concentration of GdHCl. For monolith studies, the rehydrated monolith (wet-aged or dry-aged) was mounted into a quartz cuvette and 1.30 ml of buffer was added. The 8.0 M GdHCl solution was added into the buffer as described above. After each addition, the solution was gently stirred for 20 min to allow for equilibration. Once again, a fluorescence spectrum or a steady-state anisotropy value was collected at each point for both the sample and a blank containing an identical concentration of GdHCl. The solution-based spectra were corrected for dilution factors. No dilution correction was necessary for monoliths containing protein. The intensity-based and anisotropy-based unfolding curves for these experiments were obtained as described for the thermal denaturation experiments.

The unfolding curves were fit using the equation given by Santoro and Bolen:²⁰

$$F_D = \frac{(F_N + m_N[D]) + (F_U + M_U[D])}{1 + \exp\{-(\Delta G_{\text{un}}/RT + m_G[D]/RT)\}} \quad (3)$$

where F_D is the value of the fluorescence intensity (or anisotropy) at a given concentration of denaturant, $[D]$, R is the gas constant and T is the temperature (20 °C). The remaining six terms are fitting parameters, where F_N and F_U are the values of the intensity or anisotropy extrapolated to zero concentration of denaturant for the native and unfolded states, respectively, m_N and m_U are the slopes for the dependencies of F_N and F_U on denaturant concentration, ΔG_{un} is the free energy of unfolding, and m_G is the slope describing the dependence of ΔG_{un} on denaturant concentration. The transition midpoint ($D_{1/2}$) values were calculated by dividing ΔG_{un} by $-m_G$.

Acrylamide quenching studies

Acrylamide quenching studies were done for monellin in solution and in monoliths in the presence of varying amounts of GdHCl. For proteins in solution, 2.0 ml of a 10 μM monellin solution was titrated by adding a total of 22 10 μl aliquots of 8.0 M acrylamide in buffer with continuous stirring. A fluorescence spectrum was collected from the sample and an appropriate blank after each addition. Spectra were corrected for sample dilution and were integrated as described above. For monolith studies, 2.0 ml of buffer (with or without 4.5 M GdHCl) was added to the cuvettes containing the samples and the encapsulated proteins were then titrated as described above, with an equilibration time of 20 min after each addition of quencher. No

dilution corrections were done for monolith titrations. All quenching data were analyzed using the following equation:^{14,21}

$$\frac{F_0(1-f_i)}{(F-F_0f_i)e^{V[Q]}} = 1 + K_{\text{SV}}[Q] = 1 + k_q\tau_0[Q] \quad (4)$$

where F_0 is the fluorescence intensity in the absence of the quencher, F is the fluorescence intensity at a given molar concentration of quencher $[Q]$, f_i is the fraction of monellin which is inaccessible to quencher, K_{SV} is the Stern–Volmer quenching constant (1 mol⁻¹), V represents the volume (in 1 mol⁻¹) of the active quenching sphere within which the quenching of the fluorophore is instantaneous, k_q is the bimolecular quenching rate constant (mol⁻¹ s⁻¹) and τ_0 is the unquenched fluorescence lifetime (s).

Results and discussion

Thermal stability studies

Steady-state fluorescence spectra and fluorescence anisotropy were measured at various temperatures for monellin in solution, in wet-aged monoliths and in dry-aged monoliths. The spectral characteristics at 20 °C and 70 °C are given in Table 1. The spectral characteristics of free and entrapped monellin at 20 °C were similar, although the anisotropy of the entrapped monellin was higher than in solution, probably owing to the higher viscosity of solvents within sol–gel derived matrices.^{5(b),6(a),22} This suggests that encapsulation did not induce substantial conformational changes in the native protein, and agrees with results reported for other proteins.^{2,3,14(a)}

The spectral characteristics of the denatured protein were quite different in sol–gel derived matrices when compared to the protein in solution. The spectral changes in solution were consistent with the movement of the Trp residue from a moderately hydrophobic region, which was fairly well protected from the solvent, to a more exposed and more polar environment as monellin was heated.⁷ Cooling the protein to 20 °C did not result in a full recovery of the native spectral characteristics. This was probably due to a small amount of aggregation, which was evident from the increase in light scattering at 330 nm observed for the cooled protein.

Upon encapsulation, the shifts in both the emission maximum and anisotropy values upon unfolding were significantly smaller than in solution. This is consistent with a restriction in conformational motion, and suggests that the protein either did not unfold completely or unfolded to a state which was different than that in solution. Interestingly, the decrease in intensity was greater for entrapped proteins compared to the protein in solution. Given the smaller changes in emission wavelength and anisotropy upon unfolding of entrapped proteins, the larger decreases in intensity for entrapped proteins suggest that the monoliths retained a large amount of entrapped O₂ even after purging with nitrogen, leading to an increase in the quenching of the exposed Trp residue.²³

Table 1 Fluorescence spectral and steady-state anisotropy data for thermal denaturation of monellin

Matrix	Intensity change ($\pm 2\%$) [*]	λ_{max} Native/ nm	λ_{max} Increase/ nm ^{*,†}	FWHM increase/ nm ^{*,‡}	Initial anisotropy	Decrease in anisotropy [§]
Solution	53% decrease	335 [‡]	9 [‡]	10 [‡]	0.134 ± 0.002	0.046 ± 0.004 [§]
Wet-aged	80% decrease	334	4	6	—	—
Dry-aged	60% decrease	335	4	3	0.202 ± 0.002	0.031 ± 0.004 [§]

^{*} Changes reported refer to a change in temperature from 20 °C to 70 °C for monellin in solution or wet-aged monoliths, or from 20 °C to 80 °C for monellin in dry-aged monoliths. [†] The error of each value is ± 1 nm. [‡] FWHM is full-width-at-half maximum. [§] This is the difference in anisotropy values between 45 °C and the point where aggregation begins, taken at ≈ 65 °C.

Figs. 1 and 2 show the plots of normalized integrated intensity and steady-state anisotropy at different temperatures for monellin in solution and when encapsulated. The intensity and anisotropy changes observed in the initial and final portions of the unfolding curves are due to thermally induced effects on the quantum yield and mobility of the Trp residue, and are normally observed during thermal denaturation of proteins.²⁴ The anisotropy curve for monellin in dry-aged monoliths did not show substantially sloping baselines, suggesting that increases in temperature did not affect the global motion of the folded protein when entrapped. This provides further evidence that the motions of entrapped monellin were restricted upon entrapment. In most cases, the main unfolding transition could be detected by both intensity and anisotropy changes. However, the wet-aged monoliths produced a significant degree of light scattering which could be observed using both fluorescence and absorbance measurements. The polarized nature of the scattered light resulted in extremely high anisotropy values from wet-aged monoliths.²⁵ For this reason, it was not possible to obtain meaningful data from anisotropy measurements of monellin in wet-aged monoliths.

An interesting aspect of the intensity-based thermal unfolding curves is that encapsulation of monellin into dry-aged monoliths resulted in a broadening of the unfolding transition, as shown in Fig. 1. The unfolding range was approximately 18 °C for monellin in dry-aged monoliths, while the unfolding range for monellin in solution and wet-aged monoliths was only 14 °C. This suggests that there was a distribution of microenvironments for the entrapped protein in dry-aged monoliths, each with a slightly different thermodynamic stability. This agrees with previous studies by Bright and co-workers^{6(a)} and our own group,¹³ which suggest that a distribution of environments probably exists within sol-gel derived matrices.

The intensity-based unfolding curves for free and entrapped monellin were analyzed using eqn. (1). The results are given in Table 2 for the protein at pH 7.2. Attempts to fit the anisotropy-based unfolding curves were unsuccessful, probably owing to the large increase in anisotropy above 65 °C for both free and entrapped monellin. For the free protein, it was assumed that the unfolding was a two-state reaction from a native state (N) to an unfolded state (U), and that complete unfolding occurred. In the case of entrapped proteins, it was assumed that the protein unfolded to some intermediate state (I) which may or may not be identical to the completely unfolded state obtained in solution. This intermediate state represents the final state for the denatured protein within the monoliths, and thus allows the unfolding to be treated as a two-state unfolding problem. It is realized that the values calculated for entrapped proteins using eqn. (1) probably represent the average over a distribution of environments. However, these values are still useful for the purposes of comparisons to solution values.

Two comparisons can be made to better understand the meaning of the thermodynamic data. The first is a comparison of solution values to those obtained in wet-aged monoliths. Here, the T_{un} value increased by 3 °C while both ΔH_{un}^0 and ΔS_{un}^0 decreased by about 15% upon entrapment of monellin into wet-

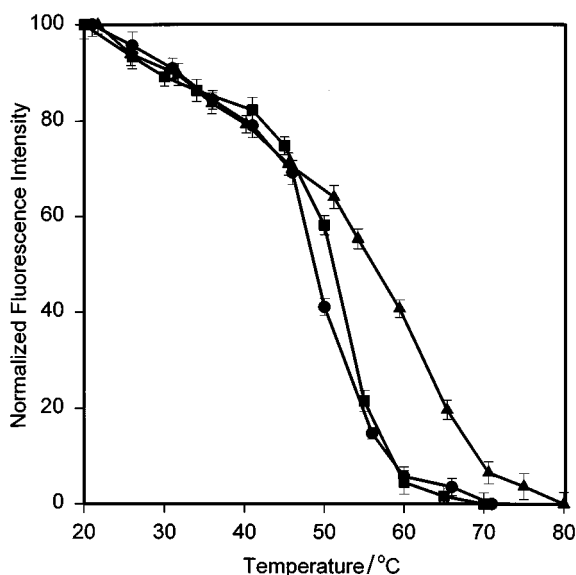


Fig. 1 Changes in fluorescence intensity for monellin as a function of temperature in solution (●); in a wet-aged monolith (■); and in a dry-aged monolith (▲). The symbols are the experimentally derived data points. The solid lines are the lines-of-best-fit as determined by fitting to eqn. (1). The data was normalized by setting the initial intensity to a value of 100 and the final intensity to a value of 0 to provide an overlap of each unfolding curve.

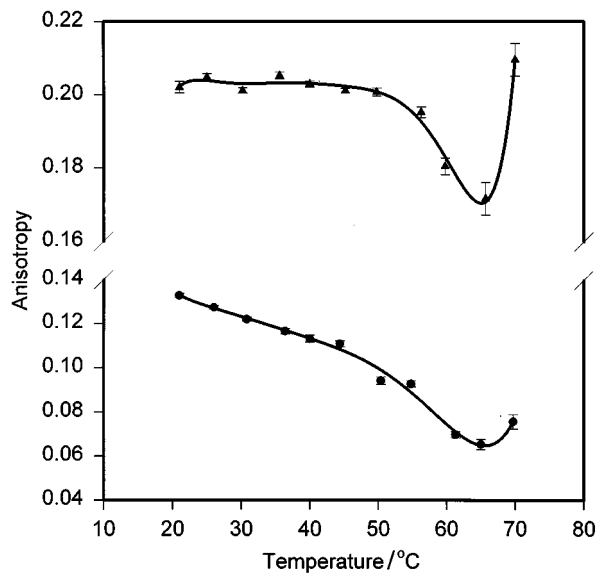


Fig. 2 Changes in fluorescence anisotropy for monellin as a function of temperature in solution (●); and in a dry-aged monolith (▲). The symbols are the experimentally derived data points. The solid lines are the lines-of-best-fit as determined by fitting to eqn. (1).

Table 2 Thermodynamic parameters for thermal unfolding of monellin in solution and in wet-aged or dry-aged monoliths

Sample	$\Delta H_{un}^0/\text{kJ mol}^{-1}$ *	$\Delta S_{un}^0/\text{J K}^{-1} \text{mol}^{-1}$ *	$T_{un}/\text{°C}^\dagger$	$\Delta G_{un}^0/\text{kJ mol}^{-1}$ ‡	χ^2 §
Monellin in solution	504 ± 50	1560 ± 125	50 ± 1	32.9 ± 4.5	0.98
Monellin in a wet-aged monolith	434 ± 45	1330 ± 120	53 ± 1	26.7 ± 3.5	0.99
Monellin in a dry-aged monolith	300 ± 28	890 ± 70	64 ± 1	9.0 ± 1.3	0.99

* These values were obtained by fitting of intensity-based unfolding curves to eqn. (1) with the following fitting parameters: solution, $F_{ON} = 100.1$, $F_{OU} = 44.2$; $s_N = -0.96$; $s_U = -0.62$. Wet-aged monolith, $F_{ON} = 99.0$; $F_{OU} = 14.6$; $s_N = -0.87$; $s_U = -0.21$. Dry-aged monolith, $F_{ON} = 99.7$, $F_{OU} = 3.7$, $s_N = -0.87$, $s_U = -0.05$. † Calculated from $\Delta H_{un}^0/\Delta S_{un}^0$. ‡ The value of ΔG_{un}^0 was determined using a value of $\Delta C_{p,un} = 10\,600 \text{ cal (deg mol)}^{-1}$.

§ Determined from non-linear curve fitting using SigmaPlot 1.02 for Windows.

aged monoliths. The lower values of ΔH_{un}^0 and ΔS_{un}^0 suggest that monellin unfolded to a different state in solution as compared to that in the monolith. The lower value for the enthalpy of unfolding can be interpreted in terms of a lower amount of heat energy being absorbed by the protein during unfolding in monoliths when compared to the protein in solution. The difference in the entropy of unfolding can be interpreted in terms of the change in the solvation of the protein upon unfolding. Generally, the unfolding of a protein will result in a large increase in the amount of water molecules required for solvation of the polypeptide backbone of the protein.^{26,27} The smaller total change in entropy for monellin in a wet-aged monolith can therefore be interpreted in terms of a lower degree of exposure of the protein backbone to solvent, which is consistent with a restriction in the conformational motions of the entrapped protein and thus a smaller degree of unfolding. The smaller changes in the enthalpy and entropy of unfolding strongly suggests that the unfolding behaviour was quite different upon entrapment, and is probably indicative of incomplete unfolding.

The second comparison that can be made is between the thermodynamic values obtained in wet-aged monoliths and those obtained in dry-aged monoliths. In this case, the ΔH_{un}^0 decreased by about 30% while the ΔS_{un}^0 value decreased by 33% compared to the values obtained from monellin in wet-aged monoliths. This has the effect of increasing the T_{un} by 11 °C (since $T_{\text{un}} = \Delta H_{\text{un}}^0 / \Delta S_{\text{un}}^0$), suggesting that the protein has increased thermal stability in dry-aged monoliths. The further decrease in the values of ΔH_{un}^0 and ΔS_{un}^0 for unfolding for monellin in dry-aged monoliths compared to wet-aged monoliths suggests that the amount of heat absorbed and the solvation of the protein by the entrapped solvent is altered, and suggests that the protein is less capable of unfolding as the monolith ages. This lower entropy value is probably a manifestation of the higher overall rigidity of solvents within dry-aged monoliths.^{3(a),13} A more rigid solvent will not undergo as large a change in entropy upon ordering of the solvent around the unfolded protein, and thus the entropy change is smaller for unfolding of the protein in dry-aged monoliths compared to wet-aged monoliths.

In order to properly calculate the free energy of the unfolding transition using eqn. (2), it was necessary to determine the change in heat capacity between the folded and unfolded states of the protein. This value was determined by monitoring the thermal unfolding of monellin in solution at different pH values and calculating ΔH_{un}^0 , ΔS_{un}^0 and T_{un} in each case. The change in heat capacity ($\Delta C_{\text{p},\text{un}}$) was determined from a plot of $\Delta(\Delta H_{\text{un}}^0)$ vs. ΔT_{un} , and had an average value of $10\,600 \pm 1500$ J (mol deg)⁻¹. This value is in reasonable agreement with values determined for other proteins of a similar size.²⁸ It was assumed that this value was similar in wet-aged and dry-aged monoliths, based on the fact that this parameter is not very solvent dependent.²⁹

The value of ΔG_{un} was determined for free and encapsulated monellin [eqn. (2)] and the values are given in Table 2. Again comparing the values obtained for monellin in solution and in wet-aged monoliths, it is apparent that the value of ΔG_{un} was lower for the entrapped protein. This is expected, given the lower values of both ΔH_{un}^0 and ΔS_{un}^0 for the entrapped protein, and is a further indication that the entrapped protein did not unfold completely. Given the likelihood of incomplete unfolding for the entrapped protein, the free energy change may not be a useful indicator of stability differences upon encapsulation. However, the unfolding temperature calculated from eqn. (1) does seem to provide a useful indication of protein stability, and suggests an overall increase in protein stability upon encapsulation into wet-aged monoliths.

The value of ΔG_{un} for the dry-aged monolith was significantly lower than the value obtained either in solution or in

wet-aged monoliths. Given the obvious increase in the temperature of the unfolding transition, it would appear that the calculated free energy value may be significantly lower than the actual value. The value of ΔG_{un} was calculated based on the assumption that $\Delta C_{\text{p},\text{un}}$ was similar in solution, wet-aged and dry-aged monoliths. Clearly, if the protein is not fully unfolding then the differential heat capacity of the folded and unfolded states will be significantly reduced. The value of ΔG_{un} was recalculated at several values of $\Delta C_{\text{p},\text{un}}$, and increased as the value of $\Delta C_{\text{p},\text{un}}$ decreased, reaching a value of 39 kJ mol⁻¹ for a $\Delta C_{\text{p},\text{un}}$ value of 0 J (deg mol)⁻¹. Since the value of $\Delta C_{\text{p},\text{un}}$ was not known for monellin in dry-aged monoliths, we were not able to reliably calculate a free energy value. For this reason, a second method of obtaining ΔG_{un} was used which had no reliance on temperature, and thus did not depend on the value of $\Delta C_{\text{p},\text{un}}$. This is described in the next section.

Overall, the thermodynamic analysis of the unfolding of monellin in solution and in wet-aged or dry-aged monoliths provided several useful pieces of information. The lowering of the enthalpy and entropy values upon entrapment clearly show that the unfolding of the entrapped protein results in a different final state compared to the free protein in solution. The thermodynamic analysis also showed that the unfolding temperature (T_{un}) of monellin was only slightly affected by encapsulation in wet-aged monoliths, but was increased by 14 °C upon entrapment in dry-aged monoliths. These results indicate that the initial stages of monolith formation did not substantially alter the stability of the protein, at least in the case of monellin. The lack of a large improvement of thermal stability in wet-aged monoliths is not unexpected since the wet-aged monoliths are still fairly loosely crosslinked.³⁰ The viscosity of the entrapped solvent within such monoliths is similar to that in solution,^{6(a)} thus the protein appears to behave as if it were in solution, although it is not able to fully unfold. The substantial increase in the unfolding temperature for monellin in dry-aged monoliths provides solid evidence that the sol-gel derived matrix dramatically alters the behaviour of the entrapped protein. This indicates that the internal environment of dry-aged monoliths is substantially different than that of aqueous solution, in agreement with our previous study.¹³

Chemical stability studies

Table 3 shows the spectral characteristics and steady-state fluorescence anisotropy values obtained from monellin in solution, wet-aged monoliths and dry-aged monoliths at different levels of the chemical denaturant GdHCl. The spectral characteristics of native monellin (no denaturant) were identical to those obtained during thermal denaturation studies. Once again, the shifts in the spectral emission maxima and anisotropy were smaller for unfolding of entrapped monellin than for the protein in solution, in agreement with the results from the thermal denaturation studies. The change in the emission maximum upon unfolding of the protein in wet-aged monoliths was slightly larger than in dry-aged monoliths, suggesting that the conformational motion of the protein was reduced upon drying, which is again in agreement with the results from the thermal denaturation study.

Figs. 3 and 4 show the integrated intensity and steady-state anisotropy at different levels of denaturant for monellin in solution and when encapsulated. In all cases, there was an initial increase in intensity. In solution, the increase was 30% during the addition of the first 1.5 M of GdHCl, while the increase was roughly half as large for the encapsulated protein. This increase was accompanied by a decrease in the accessibility of the Trp residue to the quencher acrylamide (described below), indicating that the presence of GdHCl resulted in a conformational change in the region of the Trp residue. This type of behaviour has been observed for other proteins such as ribonuclease T₁

and barnase, and has been interpreted in terms of the specific binding of guanidine to the protein, with the induction of a change in fluorescence properties.³¹ The smaller increase of intensity for the encapsulated protein suggests that either not all of the protein was accessible to GdHCl, or that the interaction of GdHCl with the entrapped protein was not able to produce as large a conformational change as was possible in solution.

Between roughly 1.5 M and 4.0 M a large decrease in intensity was observed for monellin in solution and in wet-aged monoliths. Using the intensity at 1.5 M as a basis point, it is evident that in both cases the intensity decreased by approximately the same amount, and it is apparent that the slope of the denaturation curves are quite similar. A simple visual inspection of the unfolding curves suggests that the monellin in wet-aged monoliths was not significantly stabilized compared to monellin in solution, in agreement with the thermal denaturation study. The results for denaturation of monellin in dry-aged monoliths were quite different from the results obtained in solution or wet-aged monoliths. In this case, the intensity decreased by only 20% as the concentration of GdHCl was increased from 1.5 M to 4.5 M. In addition, neither the intensity nor the emission maximum values became constant even when 5.0 M of GdHCl was present. This lends support to the suggestion that the protein may not have completely unfolded in dry-aged monoliths. The most striking aspect of the unfolding curve for monellin in dry-aged monoliths is the breadth of the unfolding

transition. This clearly shows that the protein exists in a distribution of environments, each with a slightly different thermodynamic stability, and again agrees with the results obtained from the thermal denaturation study.

The steady-state anisotropy values measured during chemical denaturation of free and entrapped monellin (Fig. 4) provided further evidence that the environment of the entrapped proteins was substantially different from a normal aqueous environment. Once again, the average anisotropy of the native protein in wet-aged and dry-aged monoliths was substantially higher than the value obtained in solution, as was observed during the thermal denaturation studies. In both solution and monoliths, the anisotropy of monellin remained relatively constant over a range of 0 M to 2.5 M GdHCl. The insensitivity of anisotropy to GdHCl concentration over this range indicates that the overall mobility of the protein in the region of the Trp residue remained constant. Further addition of GdHCl caused the anisotropy of free monellin to decrease substantially, which is indicative of an unfolded protein where the local motion of the Trp residue dominates the depolarization behaviour. For monellin in wet-aged and dry-aged monoliths, addition of GdHCl caused an obvious decrease in the anisotropy, which clearly showed the unfolding transition. However, in both cases, the change in anisotropy was significantly smaller than that obtained in solution. This result can be interpreted in several ways; incomplete unfolding of the protein, a contribution from an

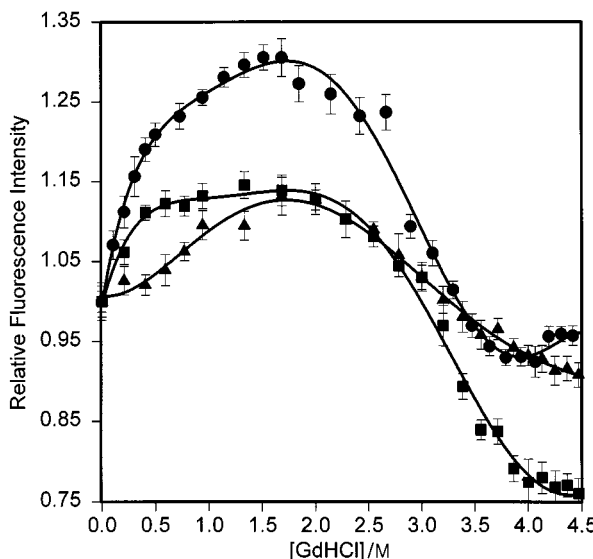


Fig. 3 Changes in fluorescence intensity for monellin as a function of GdHCl concentration in solution (●); in a wet-aged monolith (■); and in a dry-aged monolith (▲). The symbols are the experimentally derived data points. The solid lines are the lines-of-best-fit as determined by fitting to eqn. (3).

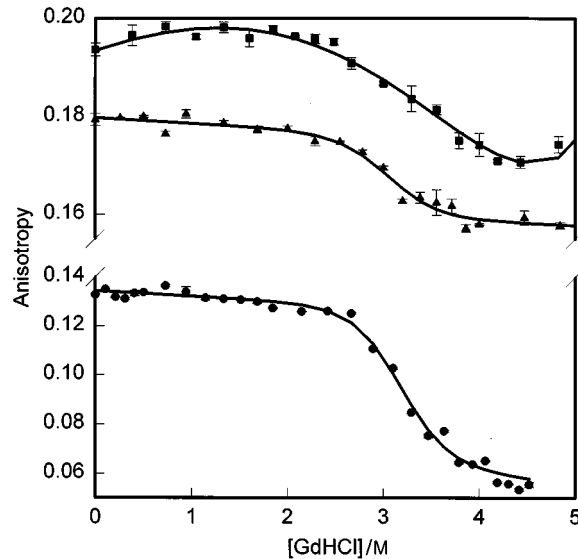


Fig. 4 Changes in fluorescence anisotropy for monellin as a function of GdHCl concentration in solution (●); in a wet-aged monolith (■); and in a dry-aged monolith (▲). The symbols are the experimentally derived data points. The solid lines are the lines-of-best-fit as determined by fitting to eqn. (3).

Table 3 Spectral data for chemical denaturation of monellin in solution, wet-aged monoliths and dry-aged monoliths

Matrix	Intensity change ($\pm 2\%$)	λ_{\max} Native/nm	λ_{\max} Increase [*] /nm	FWHM increase [†] /nm	Initial anisotropy	Decrease in anisotropy [*]
Solution	30% increase [‡] 38% decrease [§]	334 [¶]	11 [¶]	5 [¶]	0.134 ± 0.004	0.079 ± 0.007
Wet-aged monolith	15% increase 40% decrease	333	7	5	0.0195 ± 0.006	0.024 ± 0.008
Dry-aged monolith	13% increase 20% decrease	334	5	4	0.20 ± 0.006	0.023 ± 0.008

* Total change in emission wavelength or anisotropy between 0 M and 4.5 M GdHCl. † FWHM is full-width-at-half maximum. ‡ For addition of first 1.5 M GdHCl. § For addition of the next 2.5 M GdHCl. ¶ The error of each value is ± 1 nm.

inaccessible fraction of protein, an environment of higher local viscosity compared to solution; or a large contribution from scattering which leads to an apparent increase in anisotropy. Given the results presented up to this point, it is most likely that the smaller changes in anisotropy reflected a restriction of the conformational motions of the entrapped proteins, and resulted from incomplete unfolding of the entrapped protein.

To obtain quantitative information on the changes in stability upon encapsulation, the intensity and anisotropy-based unfolding curves for free and entrapped monellin were analyzed using eqn. (3). The thermodynamic data is shown in Table 4. The unfolding free energy values obtained from anisotropy data are significantly larger than those obtained from intensity data. This trend is probably the result of the inability to properly fit eqn. (3) to the intensity-based unfolding curve, owing to the initial intensity rise. This is apparent from the poorer chi-squared values and non-random residual plots (not shown) for the intensity-based data. The free energy change for the unfolding transition (calculated from anisotropy-based unfolding curves owing to the better correlation co-efficients) provides values which are in excellent agreement with the values obtained from thermal denaturation for monellin in solution and in wet-aged monoliths. However, the free energy value obtained from chemical denaturation studies of monellin in dry-aged monoliths increases slightly (compared to the value obtained for monellin in wet-aged monoliths), and is substantially higher than the value obtained from thermal denaturation experiments. This strongly suggests that the free energy value calculated for monellin in dry-aged monoliths from thermal denaturation data was significantly affected by the choice of an incorrect value for $\Delta C_{p,un}$. The slight increase in the value of ΔG_{un} for monellin as the monolith aged is in qualitative agreement with the increase in the unfolding temperature. The lower values of ΔG_{un} for entrapped monellin as compared to monellin in solution again suggests that the protein was not able to fully unfold when entrapped, and agrees with the data obtained from the thermal denaturation study.

The other important piece of information from the chemical denaturation curves is that the midpoint of the unfolding transition is similar for free and entrapped proteins. This is probably true for the protein in solution and wet-aged monoliths, given the similarity in the denaturant indices (m_G values) and the slopes of the unfolding transition, but is

Table 4 Thermodynamic parameters for the GdHCl induced unfolding of monellin

Sample	$\Delta G_{un}/$ kJ mol ⁻¹ *	$-m_G/$ kJ 1 mol ⁻² *	$D_{1/2}/$ M ^{*,†}	$\chi^2\ddagger$
Monellin in solution	$24 \pm 3\text{s}$	6.8 ± 0.7	3.0 ± 0.4	0.90
	$34 \pm 2\text{t}$	8.0 ± 0.8	3.2 ± 0.3	0.99
Molellin in a wet-aged monolith	22 ± 2	6.7 ± 0.9	3.2 ± 0.5	0.98
	27 ± 1	8.2 ± 0.8	3.3 ± 0.3	0.99
Monellin in a dry-aged monolith	20 ± 2	6.1 ± 0.5	3.2 ± 0.3	0.95
	29 ± 1	9.4 ± 0.8	3.1 ± 0.2	0.99

* The first value is that obtained from measurements of integrated intensity. The second is that obtained from measurements of steady-state anisotropy. † This value was obtained by dividing ΔG_{un} by $-m_G$. ‡ Determined from non-linear curve fitting using SigmaPlot 1.02 for Windows. § Fitting parameters from intensity measurements were as follows: solution, $F_N = 1.30$; $F_U = 0.656$; $m_N = 0.00$; $m_U = 0.068$. Wet-aged monolith, $F_N = 1.145$; $F_U = 0.766$; $m_N = 0.00$; $m_U = -0.002$. Dry-aged monolith, $F_N = 1.132$; $F_U = 1.130$; $m_N = 0.00$; $m_U = 0.051$. ¶ Fitting parameters from anisotropy measurements were as follows: solution, $F_N = 0.134$; $F_U = 0.003$; $m_N = 0.001$; $m_U = 0.012$. Wet-aged monolith, $F_N = 0.196$; $F_U = 0.154$; $m_N = 0.001$; $m_U = -0.004$. Dry-aged monolith, $F_N = 0.182$; $F_U = 0.157$; $m_N = 0.00$; $m_U = 0.001$.

probably not valid in the case where monellin is encapsulated in dry-aged monoliths. In the latter case, there is obviously a much broader unfolding transition and a higher value for the denaturant index, signifying a distribution of environments for the protein, each of which has a different thermodynamic stability. However, the fitting was done with the assumption of a single type of environment, which is certainly too simplistic based on the breadth of the unfolding transition in dry-aged monoliths.

The thermal and chemical unfolding curves for free and entrapped monellin both suggest that the protein is conformationally restricted upon entrapment and that this may lead to incomplete unfolding of the entrapped protein. These results are very interesting when one considers that chemical denaturation relies on the ability of a denaturing species to reach different parts of the protein, and thus should rely on accessibility of denaturant to different regions of the monolith, while thermal denaturation should have no dependence on protein accessibility since temperature changes should affect all proteins equally. The similarity in unfolding behaviour suggests that the ability of GdHCl to access and thus denature the protein was not significantly affected by encapsulation in wet-aged or dry-aged monoliths. These results argue against a substantial inaccessible fraction of protein in the either wet-aged or dry-aged monoliths.

Acrylamide quenching

To further explore the accessibility of the folded and unfolded protein, acrylamide quenching studies were undertaken. Fig. 5 shows typical Stern–Volmer plots of the acrylamide quenching of monellin in solution at various concentrations of GdHCl. These data were analyzed using eqn. (4). The results are shown in Table 5. The quenching of native monellin showed a K_{SV} value of 3.3 l mol^{-1} and a quenching sphere volume of 0.4 l mol^{-1} . As the concentration of GdHCl in solution was increased to 2.5 M , the K_{SV} value decreased, indicating that the environment of the Trp residue was altered as the level of denaturant increased. This correlates to the increase in the intensity observed during the intensity based titrations, and confirms that the protein undergoes a slight conformational change upon interaction with GdHCl. Increasing the denaturant

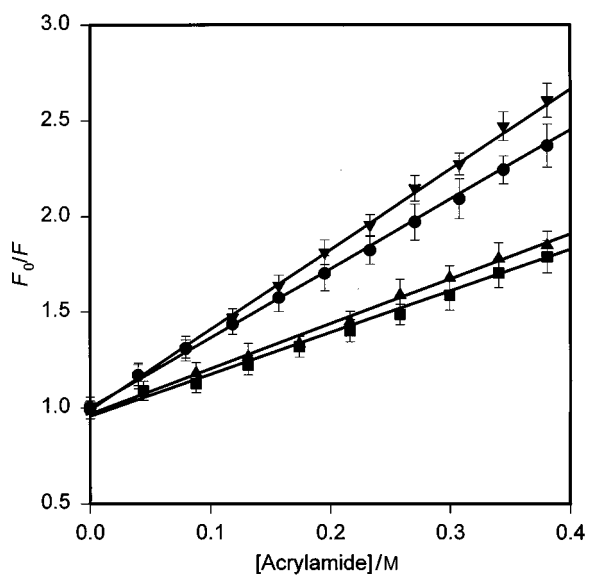


Fig. 5 Stern–Volmer plots for acrylamide quenching of monellin in aqueous buffer solution at 0 M GdHCl (●); 1.8 M GdHCl (■); 2.5 M GdHCl (▲); and 4.5 M GdHCl (▼). The data was plotted according to eqn. (4) and was fit as described in Table 5.

concentration to 4.5 M resulted in the main unfolding transition, and caused an increase in the K_{SV} value to 4.2 l mol⁻¹. In all cases the protein was fully accessible to quencher (*i.e.*, $f_i = 0$) as would be expected for a protein in solution.

The K_{SV} value is the combination of the bimolecular quenching constant (k_q) and the unquenched lifetime (τ_0). The mean fluorescence lifetime of native monellin is 2.6 ns,^{19(b)} providing a k_q value of 1.26×10^{-9} l mol⁻¹ s⁻¹. The fluorescence lifetime drops to 1.8 ns in the presence of 4.5 M GdHCl (unpublished results), resulting in a k_q value of 2.33×10^{-9} l mol⁻¹ s⁻¹, which is almost double the value of the native protein. The k_q is still substantially lower than that of free tryptophan ($k_q = 5.86 \times 10^{-9}$ l mol⁻¹ s⁻¹),^{19(a)} but this is expected owing to the presence of the polypeptide chain which will partially block the accessibility of acrylamide to the Trp in the protein. These results therefore indicate that the Trp does become substantially more exposed upon denaturation with GdHCl.

Table 6 shows the values obtained from Stern–Volmer analysis of monellin in wet-aged and dry-aged monoliths, with the data fit according to eqn. (4). In all cases, the equation provided an excellent fit to the data, with correlation coefficients of 0.98 or better, as shown in Table 6. The quenching experiments for the encapsulated proteins were performed only at 0 M and 4.5 M GdHCl to provide an overview of the changes incurred by the presence of the denaturant. Acrylamide quenching of native monellin in a wet-aged and dry-aged monolith indicated that the K_{SV} value dropped upon encapsulation, while the quenching sphere volume remained relatively constant. In addition, entrapment caused the fraction of inaccessible protein to increase to between 8% and 15%. The K_{SV} values in the presence of 4.5 M GdHCl were similar or less than to those in the absence of denaturant, while the V values increased slightly and the f_i values decreased slightly (for monellin in wet-aged monoliths).

It is interesting to note that monellin in both wet-aged and dry-aged monoliths at 4.5 M GdHCl had quenching results which were almost identical to those for monellin in solution at 2.5 M GdHCl. These results strongly suggest that the protein did not fully unfold when entrapped, and ended up in a conformation which was similar to that of partially denatured monellin in solution. These results are in agreement with both the smaller change in the emission maximum and the smaller change in anisotropy upon thermal or chemical unfolding of the entrapped protein. This is not surprising given that the average pore size of the dry-aged monoliths was 6.7 nm,¹³ which is only slightly larger than the size of the folded protein (3.5 nm). Hence the restriction in conformational motions is most likely due to the steric restrictions imposed by the pore dimensions.

Table 5 Stern–Volmer analysis of acrylamide quenching for native and partially denatured monellin in solution

[GdHCl]/M	K_{SV} /l mol ⁻¹	V /l mol ⁻¹	Constant	r^2
0	3.3 ± 0.1	0.4 ± 0.01	1.01 ± 0.02	1.00
1.8	2.2 ± 0.1	1.0 ± 0.1	0.96 ± 0.01	0.99
2.5	2.4 ± 0.1	0.9 ± 0.1	0.97 ± 0.02	0.99
4.5	4.2 ± 0.2	0.9 ± 0.1	0.98 ± 0.02	1.00

The fractional inaccessibility values obtained from our quenching experiments suggest that only a small amount of protein was completely inaccessible (less than 15%). Interestingly, drying of the monolith appears to decrease the inaccessible fraction of protein. The reason for this finding is not completely clear to us, however it may be the result of the dry-aged monoliths having a cross-section which was approximately 10-fold thinner than the wet-aged monoliths.¹³ Our fractional inaccessibility values are significantly lower than those reported by Saavedra and co-workers, who studied the quenching of entrapped BSA.¹⁴ The basis for this finding is not fully understood; however, it may be partially due to several factors such as: the smaller size of monellin as compared to BSA, resulting in a lower likelihood that the protein can completely fill the pore within which it resides; the presence of two Trp residues within BSA which may have resulted in non-linear SV plots, making it more difficult to fit the data using Stern–Volmer plots;³² differences in the type of equation used to fit the quenching data; or differences in the type of denaturant (neutral in our studies *versus* negatively charged in the study by Saavedra and co-workers). Previous studies have clearly shown that the interaction between entrapped proteins and charged reagents is seriously affected by the charge on the silicate matrix.¹³ Therefore, it is possible that the entrapped proteins are inaccessible only to negatively charged quenchers, and are significantly more accessible to neutral quenchers.

Long term stability

To further investigate protein stability in TEOS monoliths, the long term stability of monellin was examined. Fluorescence spectra were collected daily over a period of several weeks until there were obvious signs of protein denaturation such as a redshift in the emission maximum or an increase in the spectral full-width-at-half-maximum (FWHM) value. Complementary absorbance studies were performed to examine scattering which would indicate protein aggregation and/or adsorption. The studies indicated that monellin in solution remained stable for 9 d prior to aggregation. However, even after 7 d, the FWHM of the fluorescence spectrum had increased and the emission maximum began to shift. Encapsulation of monellin in wet-aged monoliths caused the protein to retain native spectral characteristics for 40 d, at which time scattering became evident. In dry-aged monoliths which were aged in air for 4 weeks and then soaked in buffer continuously after aging, there were no changes in the fluorescence spectrum of monellin over a period of 12 weeks from the date of encapsulation. However, during the thirteenth week, there were signs of scattering, even though there were no observable differences in the fluorescence spectra compared to those initially obtained from dry-aged monoliths (4 weeks old). These results suggest that there is better than a 10-fold increase in protein stability upon encapsulation into dry-aged monoliths.

At first it is not apparent why the long-term stability of monellin should be improved in both wet-aged and dry-aged monoliths, even though free energy of unfolding decreased in both systems (compared to solution) and the T_{un} value was not improved in wet-aged monoliths. This behaviour indicates that the loss of structure over time is most likely determined by

Table 6 Stern–Volmer analysis of acrylamide quenching for native and chemically denatured monellin in wet-aged and dry-aged TEOS monoliths

Sample	[GdHCl]/M	K_{SV} /l mol ⁻¹	V /l mol ⁻¹	f_i	Constant	r^2
Monellin (wet-aged monolith)	0	2.3 ± 0.2	0.4 ± 0.1	0.15 ± 0.02	0.96 ± 0.01	0.98
	4.5	2.3 ± 0.2	0.9 ± 0.1	0.12 ± 0.01	0.94 ± 0.02	0.98
Monellin (dry-aged monolith)	0	2.9 ± 0.3	0.6 ± 0.1	0.08 ± 0.01	0.97 ± 0.01	1.00
	4.5	2.5 ± 0.2	1.2 ± 0.2	0.08 ± 0.01	0.97 ± 0.01	0.99

aggregation, which is possible in solution but is curtailed in both types of monoliths. Hence, even though the unfolding temperature was not significantly improved for monellin in wet-aged monoliths, the reduction in protein mobility (especially between pores) resulted in a decrease in protein aggregation, as demonstrated by the lower degree of light scattering for entrapped monellin as compared to dissolved monellin after storage.

Basis of the stability enhancement

The fluorescence results clearly showed that the entrapped protein retained the ability to undergo both thermally and chemically induced conformational changes, although the extent of such conformational changes was restricted as the monoliths aged. Aging also had a beneficial effect on the unfolding temperature of the protein, suggesting that the lower degree of conformational flexibility may be related to increased thermal stability. This suggests that the basis for the enhancement of protein stability may, in part, be the result of a simple steric restriction on the motion of the protein, with the silane 'trapping' the protein in an active conformation.^{2(b),3(a)} The exact mechanism by which the restricted mobility is related to enhanced stability is not fully understood, although it seems likely that the lower degree of mobility may hinder the movement of the protein into thermodynamically unfavourable conformations.

One possible explanation for the enhanced thermal stability comes from the changes in the ΔS_{un} value upon entrapment. It is likely that the stabilization is aided by highly structured water which surrounds the protein in the pores of the silane. The structured water may be templated through hydrogen bonding interactions with the polyhydroxylated silane. Both fluorescence^{5(a),33} and NMR^{21(a,b)} studies have shown that the mobility of entrapped solvents is lower than that of free solvents. Previous results from our group¹³ and others^{5(a)} also suggest that the viscosity of the entrapped solvent is higher in dry-aged monoliths than in wet-aged monoliths or solution. This provides evidence that the internal environment of the monoliths is more highly structured and thus less mobile than aqueous solvent.²¹ This is also supported by a recent report from Bright and co-workers which shows that the dipolar relaxation time for encapsulated solvents is slower than for free solvents.^{5(b),33} The more 'structured' solvent within dry-aged monoliths may not be as capable as 'free' solvent of adapting to a new protein conformation or of solvating exposed hydrophobic regions of proteins, leading to an overall decrease in ΔS_{un} and the higher T_{un} for the entrapped protein protein which is reported herein.

Conclusions

This report shows that monitoring of intrinsic fluorescence can provide an abundance of information about the environment and conformational motions of entrapped proteins which contain a single tryptophan residue. In addition, the thermodynamic treatment of thermal and chemical denaturation curves derived from fluorescence measurements can provide useful information regarding the stability and unfolding behaviour of entrapped proteins. This is the first report of a thermodynamic study of protein stability within sol-gel derived matrices, and has resulted in several interesting findings. Firstly, the changes in fluorescence properties with increased temperature or denaturant concentration indicate that entrapped proteins have a reduced degree of conformational flexibility upon entrapment, and that this restriction in motion may increase as the monoliths age. Secondly, denaturation results indicated that entrapment in

dry-aged monoliths resulted in a distribution of microenvironments, each having a different thermodynamic stability. Finally, the results showed that the thermal and long-term stability of the protein improved as the monoliths dried.

Preliminary results suggest that the stabilizing effect observed upon encapsulation was possibly the result of the ability of the silane to restrict the conformational flexibility of the protein, and to promote structural rigidity in the internal water. Future studies will include investigation of role of additives such as polyethylene glycol on the stability of entrapped proteins, an examination of time-resolved fluorescence data from entrapped proteins, and the use of other single Trp proteins of varying size and stability to further understand the internal environment of sol-gel derived matrices.

The authors thank the National Sciences and Engineering Research Council of Canada for financial support of this work.

References

- 1 Braun, S., Rappoport, S., Zusman, R., Avnir, D., and Ottolenghi, M., *Mater. Lett.*, 1990, **10**, 1.
- 2 (a) Nishida, F., McKiernan, J. M., Dunn, B., Zink, J. I., Brinker, C. J., and Hurd, A. J., *J. Am. Ceram. Soc.*, 1995, **78**, 1640; (b) Ellerby, L. M., Nishida, C. R., Nishida, F., Yamanaka, S. A., Dunn, B., Valentine, J. S., and Zink, J. I., *Science*, 1992, **255**, 1113.
- 3 (a) Dave, B. C., Dunn, B., Valentine, J. S., and Zink, J. I., *Anal. Chem.*, 1994, **66**, 1120A; (b) Avnir, D., Braun, S., Lev, O., and Ottolenghi, M., *Chem. Mater.*, 1994, **6**, 1605; (c) Yamanaka, S. A., Dunn, B., Valentine, J. S., and Zink, J. I., *J. Am. Chem. Soc.*, 1995, **117**, 9095.
- 4 (a) Braun, S., Rappoport, S., Zusman, R., Shteltzer, S., Drukman, S., Avnir, D., and Ottolenghi, M., in *Biotechnology: Bridging Research and Applications*, ed. Kamely, D., Chakrobary, A., and Kornguth, S. E., Kluwer Academic Publishers, Amsterdam, 1991, p. 205; (b) Heichal-Segai, O., Rappoport, S., and Braun, S., *Biotechnology*, 1995, **13**, 798; (d) Reetz, M. T., Zonta, A., and Simpelkamp, J., *Angew. Chem., Int. Ed. Engl.*, 1995, **34**, 301.
- 5 (a) Dave, B. C., Soyez, H., Miller, J. M., Dunn, B., Valentine, J. S., and Zink, J. I., *Chem. Mater.*, 1995, **7**, 1431; (b) Jordan, J. D., Dunbar, R. A., and Bright, F. V., *Anal. Chem.*, 1995, **67**, 2436.
- 6 (a) Narang, U., Jordan, J. D., Bright, F. V., and Prasad, P. N., *J. Phys. Chem.*, 1994, **98**, 8101; (b) Narang, U., Bright, F. V., and Prasad, P. N., *Appl. Spectrosc.*, 1993, **47**, 229; (c) Matsui, K., Matsuzuka, T., and Fujita, H., *J. Phys. Chem.*, 1989, **93**, 4991.
- 7 Eftink, M. R., in *Methods of Biochemical Analysis: Protein Structure Determination*, ed. Suelter, C. H., Wiley, New York, 1991, vol. 35, pp. 127-206.
- 8 (a) Dahms, T. E. S., Willis, K. J., and Szabo, A. G., *J. Am. Chem. Soc.*, 1995, **117**, 2321; (b) Dahms, T. E. S., and Szabo, A. G., *Biophys. J.*, 1995, **69**, 569.
- 9 Demchenko, A. P., Gryczynski, I., Gryczynski, Z., Wiczek, W., Malak, H., and Fishman, M., *Biophys. Chem.*, 1993, **48**, 39.
- 10 Hargrove, M. S., Krzywda, S., Wilkinson, A. J., Dou, Y., Ikeda-Saito, M., and Olson, J. S., *Biochemistry*, 1994, **33**, 11 767.
- 11 Eftink, M. R., *Biophys. J.*, 1994, **66**, 482.
- 12 Beechem, J. M., *Proc. SPIE*, 1992, **1640**, 676.
- 13 Zheng, L., Reid, W. R., and Brennan, J. D., *Anal. Chem.*, 1997, **69**, 3940.
- 14 (a) Edmiston, P. L., Wambolt, C. L., Smith, M. K., and Saavedra, S. S., *J. Colloid Interface Sci.*, 1994, **163**, 395; (b) Wambolt, C. L., and Saavedra, S. S., *J. Sol-Gel Sci. Tech.*, 1996, **7**, 53.
- 15 (a) Morris, J., and Cagan, R. H., *Biochim. Biophys. Acta*, 1972, **261**, 114; (b) Van der Wel, H., *FEBS Lett.*, 1972, **21**, 88.
- 16 Van der Wel, H., and Loeve, K., *FEBS Lett.*, 1973, **29**, 181.
- 17 (a) Ogata, C., Hatada, M., Tomlinson, G., Shin, W.-C., and Kim, S.-H., *Nature (London)*, 1987, **328**, 739; (b) Somoza, J. R., Jiang, F., Liang, T., Kang, C.-H., Cho, J. M., and Kim, S.-H., *J. Mol. Biol.*, 1993, **234**, 390.
- 18 Brand, J. G., and Cagan, R. H., *Biochim. Biophys. Acta*, 1977, **493**, 178.

19 Pace, C. N., Shirley, B. A., and Thomson, J. A., in *Protein Structure and Function: A Practical Approach*, ed. Chreighton, T. E., IRL Press Oxford, 1989, pp. 311–330.

20 Santoro, M. M., and Bolen, D. W., *Biochemistry*, 1988, **27**, 8063.

21 (a) Eftink, M. R., and Ghiron, C. A., *Biochemistry*, 1976, **15**, 672; (b) Eftink, M. R., and Ghiron, C. A., *Biochemistry*, 1977, **16**, 5546; (c) Eftink, M. R., and Ghiron, C. A., *Biochim. Biophys. Acta*, 1987, **916**, 343.

22 (a) Xu, S., Ballard, L., Kim, Y. J., and Jonas, J., *J. Phys. Chem.*, 1995, **99**, 5787; (b) Korb, J.-P., Delville, A., Xu, S., Demeulenaere, G., Costa, P., and Johas, J., *J. Chem. Phys.*, 1994, **101**, 7074; (c) Shen, C., and Kostic, N. M., *J. Am. Chem. Soc.*, 1997, **119**, 1304.

23 Lakowicz, J. R., and Weber, G., *Biochemistry*, 1973, **18**, 4161.

24 Kirby, E. P., and Steiner, R. F., *J. Phys. Chem.*, 1970, **74**, 4480.

25 Lakowicz, J. R., *Principles of Fluorescence Spectroscopy*, Plenum Press, New York, 1983, pp. 129–134.

26 Liu, Y., and Bolen, D. W., *Biochemistry*, 1995, **34**, 12 884.

27 Privolov, P. L., *Annu. Rev. Biophys. Chem.*, 1989, **18**, 47.

28 Eftink, M. R., Ghiron, C. A., Kautz, R. A., and Fox, R. O., *Biochemistry*, 1991, **30**, 1193.

29 Privolov, P. L., and Khechinashvili, N. N., *J. Mol. Biol.*, 1974, **86**, 665.

30 (a) Brinker, C. J., and Scherer, G. W., *Sol–Gel Science*, Academic Press, New York, 1989; (b) Hench, L. L., and West, J. K., *Chem. Rev.*, 1990, **90**, 33.

31 Pace, C. N., Laurents, D. V., and Thomson, J. A., *Biochemistry*, 1990, **29**, 2564.

32 Lehrer, S. S., *Biochemistry*, 1971, **10**, 3254.

33 Lundgren, J. S., Heitz, M. P., and Bright, F. V., *Anal. Chem.*, 1995, **67**, 3775.

Paper 8/00710A

Received January 26, 1998

Accepted May 15, 1998